J Mater Sci: Mater Electron (2010) 21:1262–1269
DOI 10.1007/s10854-010-0059-1

Preparation, electrocatalytic and photocatalytic performances of nanoscaled CuO/Co_3O_4 composite oxides

Lu Pan · Zude Zhang

Received: 6 July 2009 / Accepted: 13 January 2010 / Published online: 26 January 2010

Abstract Cu-Co composite oxides with different Cu/Co atomic ratios were prepared by the calcination of the precursors synthesized via a co-precipitation method. The samples were characterized by XRD, SEM and TEM, respectively. The XRD analysis revealed that only spinel structure of Cu-Co composite oxide was confirmed with lower Cu/Co ratio (<1:2). The sizes and morphologies of samples are controlled significantly by the Cu/Co atomic ratios. The electrocatalytic activity for *p*-nitrophenol reduction in a basic solution with the samples decorated on glassy carbon (GC) electrodes was tested by cyclic voltammetry (CV). The results showed that the sample with Cu/Co ratio of 2:8 exhibited the highest catalytic activity for *p*-nitrophenol reduction. The photocatalytic performances of the samples for the degradation of methyl orange under irradiation of visible light were investigated. The samples with Cu/Co ratios from 5:5 to 10:0 all showed better photocatalytic activities for methyl orange degradation, but the sample with Cu/Co ratio of 9:1 exhibited much higher catalytic activity. The catalyst with Cu/Co ratio of 9:1 also exhibited excellent repeatability for the catalytic degradation of methyl orange.

L. Pan · Z. Zhang (✉)
Department of Chemistry, University of Science and Technology of China, Hefei, Anhui 230026, China
e-mail: zhzude@163.com

L. Pan
Department of Chemistry and Chemical Engineering, Huainan Normal Univeristy, Huainan, Anhui 232001, China

1 Introduction

Copper and cobalt oxides, which both are important *p*-type semiconductor, have been investigated extensively recently. CuO, with a narrow band gap (1.21 eV) [1], has interesting photovoltaic, electrochemical, and catalytic properties [2–4], and is widely used as catalysts, gas sensors, varistors, magnetic storage media, solar cells, and cathode materials [5–8]. Co_3O_4, with direct optical band gaps at 1.48 and 2.19 eV [9], has a stable normal spinel structure of AB_2O_4 type, where Co^{2+} ions occupy the tetrahedral 8a sites and Co^{3+} occupy the octahedral 16d sites [10]. Co_3O_4 has been investigated extensively as promising materials in gas-sensing and solar energy absorption and as an effective catalyst in environmental purification and chemical engineering [11, 12]. In addition, Co_3O_4 has been widely studied for its application as lithium–ion battery electrodes, catalysts, ceramic pigments, field-emission materials and magnetic material [13–18].

Cu-M (transition metals) composite oxides have been studied extensively as catalysts for CO oxidation, such as $CuO\text{-}CeO_2$ [19, 20], $CuO\text{-}Co_3O_4$ [21], and $CuO\text{-}TiO_2$ [22]. Besides serving as the catalyst for CO oxidation, Cu-Co composite oxides have been investigated as anode for lithium–ion batteries [23, 24]. In addition, CuO and Co_3O_4 nanoparticles were used as photocatalysts for chemical pollutants degradation [4, 25]. Up to now, scarce reports have involved in the electro- and photo-catalytic performances of Cu-Co composite oxides. In this work, we have synthesized Cu-Co composite oxides with Cu/Co atomic ratios ranging from 0:10 to 10:0 via an easily controlled and inexpensive method. The electrocatalytic activities of the samples with Cu/Co ratios from 0:10 to 3:7 decorated on a glassy carbon (GC) electrode was tested, and its electrocatalytic activity for *p*-nitrophenol reduction was

much better than that of bare GC electrode in a basic solution. The photocatalytic properties for the degradation of methyl orange with the assist of H_2O_2 under visible light using the samples with Cu/Co ratios from 5:5 to 10:0 were investigated, and the results indicated that the as-prepared samples exhibited excellent photocatalytic activity for methyl orange degradation.

2 Experimental details

2.1 Preparation of CuO/Co_3O_4

The precursors of CuO/Co_3O_4 composite oxide nanoparticles with different Cu/Co atomic ratios were prepared via a co-precipitation method. Typically, 10 mmol of mixture composed of $CoC1_2{\cdot}6H_2O$ and $CuSO_4{\cdot}5H_2O$ with Cu/Co atomic ratios ranging from 0:10 to 10:0 was dissolved in 40 mL distilled water in a beaker, then 40 mL of solution containing 15 mmol NH_4HCO_3 and 20 mmol $(CH_2)_6N_4$ acted as precipitation reagent was added by dropwise under vigorous stirring. After addition of the solution, the beaker was stood for 6 h, finally was placed in 80 °C water bath for 6 h. The precipitation was filtered off and washed several times first with distilled water then with absolute ethanol. The as-prepared precipitation was dried at 105 °C for 6 h in an oven. The Cu-Co composite oxide samples were obtained by the calcination of the dried precursor in air at 400 °C for 3 h according to the TG analysis of the precursor. .

2.2 Sample characterization

Morphologies of the precursors were observed with scanning electron microscopy (SEM, KYKY- EM 3200). Phase identification was carried out by X-ray diffraction on a Philips X'Pert SUPER powder X-ray diffraction with Cu Kα radiation ($\lambda = 1.5418$ Å). The transmission electron microscopy (TEM) images were taken on Hitachi model H-800 transmission electron microscope with tungsten filament using an acceleration voltage of 200 kV. N_2 adsorption of the as-prepared samples was determined by BET measurements using a NOVA-1000e surface analyzer, and the surface area of Co_3O_4, CuO and CuO/Co_3O_4 samples are presented in Table 1.

2.3 Electrochemical property measurement

The electrochemical property measurements of the CuO-Co_3O_4/GCEs were carried out on LK 98 microcomputer-based electrochemical system. (Tianjin Lanlike Chemical and Electron High Technology Co, Ltd., Tianjin in China). A three-electrode single compartment cell was used for cyclic voltammetry. A glassy carbon (GC) electrode (3.7 mm diameter) was used as working electrode and a platinum plate used as counter electrode and a Ag/AgC1 electrode used as reference electrode. Prior to each measurement, the GC electrode surface was carefully polished on an abrasive paper first, then further polished with 0.3 and 0.05 μm α-Al_2O_3 (Buehler) paste in turn, finally rinsed thoroughly with 1:1 (v:v) HNO_3 aqueous solution, acetone and doubly distilled water and dried in the air. A total of 20 mg of CuO/Co_3O_4 sample was dispersed in 4 mL doubly distilled water under an ultrasonic treatment to obtain a black suspension solution. Of the solution, 50 μL was taken out and trickled on the carbon surface of the GC electrode. After being dried in the air, the modified GC electrode was prepared and used directly for electrochemical measurements.

Table 1 BET surface areas of as-prepared samples

Material (Cu/Co molar ratio)	BET surface area (m^2/g)
Co_3O_4 (0:10)	32
CuO/Co_3O_4 (1:9)	41
CuO/Co_3O_4 (2:8)	53
CuO/Co_3O_4 (3:7)	59
CuO/Co_3O_4 (5:5)	53
CuO/Co_3O_4 (6:4)	52
CuO/Co_3O_4 (8:2)	57
CuO/Co_3O_4 (9:1)	82
CuO (10:0)	87

2.4 Photocatalytic properties of CuO/Co_3O_4

The photocatalytic degradation experiments for methyl orange were carried out in a self-prepared reactor. In a typical degradation procedure, a certain weight amount of CuO/Co_3O_4 catalyst was dispersed in a 250 mL beaker containing 200 mL of wastewater (initial methyl orange concentration was fixed at 20 mg L^{-1}) under ultrasonic treatment for 30 min by keeping from irradiation of light. Before the solution was irradiated by a 200 W incandescent lamp, the vertical distance between the level of the solution and the horizontal plane of the lamp was fixed at 10 cm. As soon as irradiation began, 0.5 mL of oxydol solution (30%, m/v) was added to the beaker, and the wastewater was stirred vigorously. At an interval of 20 min, 3 mL of sample was taken out from the reactor and centrifuged for analytical determination. The absorbance of the sample was determined on a UV–Vis absorption photometer (T6, Puxitongyong analytic apparatus Ltd. Inc., Beijing, China) worked at 464 nm wavelength. The residual concentration of methyl orange in the wastewater was

obtained according to a working curve. When the degradation reaction was finished, the beaker was placed in a magnetic field, and the catalyst was recovered for reusing. The degradation rate of methyl orange (η) was calculated as the equation:

$$\eta = \frac{C_0 - C_t}{C_0} \times 100$$

where C_0 is the initial concentration of methyl orange; C_t concentration of methyl orangeat any time 't'.

3 Results and discussions

3.1 SEM images of precursors

Morphology of the precursors with Cu/Co atomic ratios of 1:9, 5:5 and 9:1, respectively was revealed by SEM as shown in Fig. 1. The precursors shown in Fig. 1a, b were amorphous particles and of sizes of approximate several hundreds nm. The mean sizes of the particles in Fig. 1a are larger than that of the ones in Fig. 1b. The precursor exhibited in Fig. 1c was sheet-like shape, and was piled up by a great deal of irregular little sheets with various sizes. Manifestly, the precursor with different Cu/Co ratios exhibited different morphology. The SEM images of the precursors suggested that the morphology of the resultant sample obtained by the calcination of the corresponding precursor could be nanoparticles at low Cu/Co ratios but nanosheets at higher Cu/Co ones.

3.2 TG-DTA analysis

Figure 2 shows the TA-DTA curves of the precursor of CuO/Co_3O_4 samples with Cu/Co ratio of 5:5. Two broad endothermic peaks at 190–297 and 297–370 °C, accompanied with two obvious weight losses, are observed clearly. The reduction of the sample's weight in the intervals of 190–297 °C and 297–370 °C are indicative of isolation of oxygen to obtain Co_3O_4 and CuO, respectively [26]. The weight of the sample is constant in the range

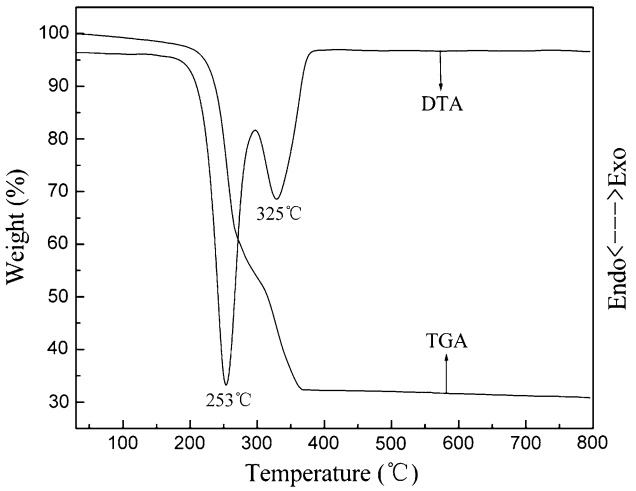

Fig. 2 TGA-DTA curves of the precursors of CuO/Co_3O_4 sample with Cu/Co atomic molar ratio of 5:5

370–800 °C which indicates that no obvious amounts of any other volatile impurities are present. To obtain the CuO/Co_3O_4 samples, the corresponding precursors were calcined at 400 °C for 3 h.

3.3 XRD patterns of samples

Figure 3 displays the XRD pattern of the CuO/Co_3O_4 composite oxides with different Cu/Co ratios along with Co_3O_4. All the diffraction peaks of Co_3O_4 can be ascribed to the cubic spinel structure of Co_3O_4. For the sample with Cu/Co ratio of 2:8, the strong diffraction peaks ascribed to the spinel phase of Co_3O_4 could be observed distinctly, and nearly no diffraction peaks ascribed to monoclinlic tenorite structure of CuO phase could be observed. The diffraction peaks with broader width indicates the crystallite sizes of CuO/Co_3O_4 composite oxides become smaller. By further increasing Cu/Co ratio to 5:5, the diffraction peaks attributed to Co_3O_4 and CuO were both detected. As Cu/Co ratio increased to 8:2, only monoclinlic tenorite structure of CuO phase could be observed. Figure 4 shows the XRD pattern of the CuO sample with monoclinlic tenorite structure.

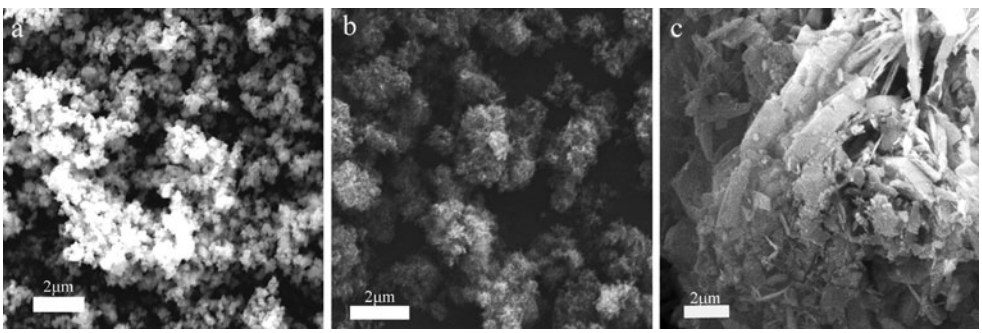

Fig. 1 SEM images of the precursors of the samples with Cu/Co ratio of **a** 1:9, **b** 5:5 and **c** 9:1

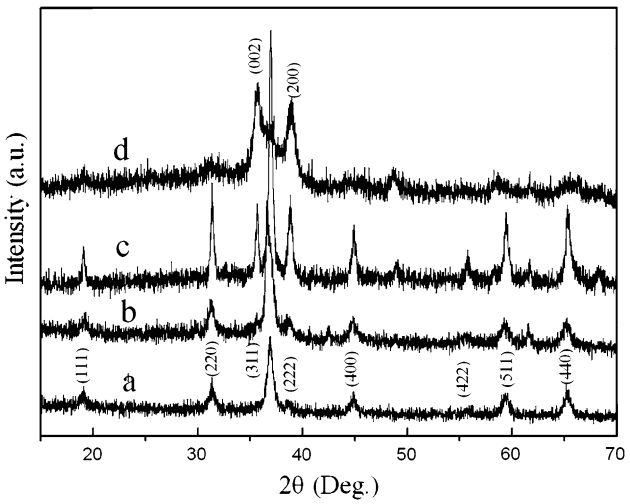

Fig. 3 X-ray diffraction patterns of samples, **a** Co_3O_4, **b–d** CuO/Co_3O_4 with Cu/Co ratio of 2:8, 5:6 and 8:2, respectively

Thus, CuO/Co_3O_4 samples can be obtained by the calcination of the precursors at no less than 400 °C for 3 h in air.

As mentioned in introduction, tricobalt tetraoxide (Co_3O_4) is described by a formula unit AB_2O_4 (A → Co^{2+}, B → Co^{3+}) and exhibits a normal spinel crystal structure with occupation of tetrahedral A sites by Co^{2+} and octahedral B sites by Co^{3+} in cubic closely-packed structure of O^{2-}, where the ratio of Co^{3+}/Co^{2+} is 2:1. As Cu^{2+} possesses the ionic charge and similar ionic diameter ($D_{Cu}2+=73$ pm) to Co^{2+} ($D_{Co}2+=74.5$ pm), it is reasonable to speculate that Cu^{2+} could replace Co^{2+} entering the cubic structure of Co_3O_4, and a composite spinel structure of $Cu_xCo_{3-x}O_4$ could be formed. If Co^{2+} in Co_3O_4 was replaced totally by Cu^{2+}, the maximum number of Cu^{2+} accommodated by $Cu_xCo_{3-x}O_4$ with spinel structure was at Cu/Co ratio of 1:2

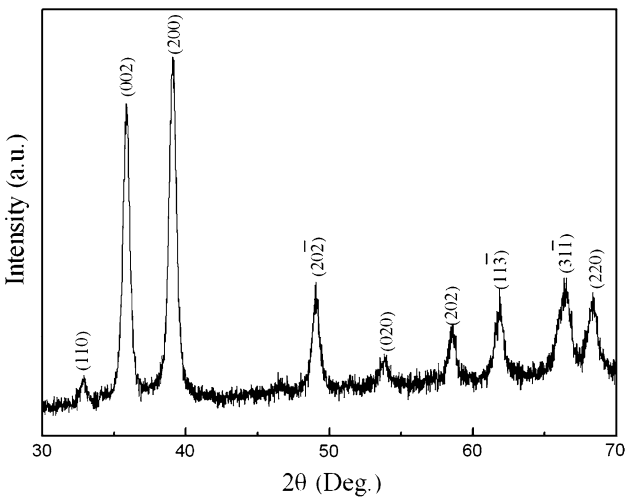

Fig. 4 X-ray diffraction pattern of CuO

[21]. According to XRD pattern of CuO/Co_3O_4 composite oxide with Cu/Co ratio of 2:8, nearly no diffraction peaks of CuO could be observed, which revealed that $Cu_xCo_{3-x}O_4$ with spinel structure was possible formed in the sample.

3.4 TEM images of samples

Morphology of the CuO/Co_3O_4 samples with different Cu/Co atomic ratios was demonstrated by TEM shown in Fig. 5. For Co_3O_4 (Fig. 5a), the product was nanoparticles with mean size of approximate 25 nm. By increasing Cu/Co ratio to 2:8, the CuO/Co_3O_4 sample was still nano-sized particles but with smaller size (mean size was approximate 15 nm) (Fig. 5b), which was in good agreement with the XRD analysis of CuO/Co_3O_4 samples. With further increase of the Cu/Co ratio to 5:5 and 6:4, the size of CuO/Co_3O_4 nanoparticle further decreased and only was about 10 nm, and obvious aggregation of particles were observed (Fig. 5c and d). When the Cu/Co ratio increased to 7:3, the size of the sample increased and a few sheet-like products, which could be piled up by smaller sized CuO/Co_3O_4 nanoparticle, was observed (Fig. 5e). Further increasing Cu/Co ratio to 9:1 and 10:0, the resultant samples with sheet-like shape were obtained (Fig. 5f and g). One can find out that the samples have numerous micropores, which is favorable for enhancing the specific surface areas. Based on TEM images in Fig. 5, with a lower Cu/Co ratio, the CuO/Co_3O_4 sample was in good dispersion, and with a higher Cu/Co ratio, CuO/Co_3O_4 nanoparticles was inclined to aggregate until form nanosheets.

3.5 Electrocatalytic performances of samples

Cyclic voltammograms of bare GC electrode and GC electrode modified with different CuO, Co_3O_4 and CuO/Co_3O_4 samples with different Cu/Co ratios in presence of *p*-nitrophenol in a basic solution are shown in Fig. 6. When a bare GC electrode was used, the electrocatalytic activity for *p*-nitrophenol reduction was low, only with a current peak value of 40.07 μA at a potential of −1.044 V, as curve (1) in Fig. 6. Thus the bare GC electrode demonstrated poor electocatalytic activity for the *p*-nitrophenol reduction in base solution. When the GC electrode modified with Co_3O_4 was used, the reduction reaction could be carried out at a potential of −1.020 V with a larger current peak value of 115.57 μA, no oxidation peak could be observed, as curve (2) in Fig. 6. When the GC electrode modified with CuO/Co_3O_4 samples with Cu/Co ratios of 1:9, 2:8 and 3:7, respectively were used, correspondingly two, three and two reduction peaks in curve (3), (4) and (5), respectively were observed, but each oxidation peak in curve (3), (4) and (5) was detected as shown in Fig. 6. The peak potential value vs. peak current value was

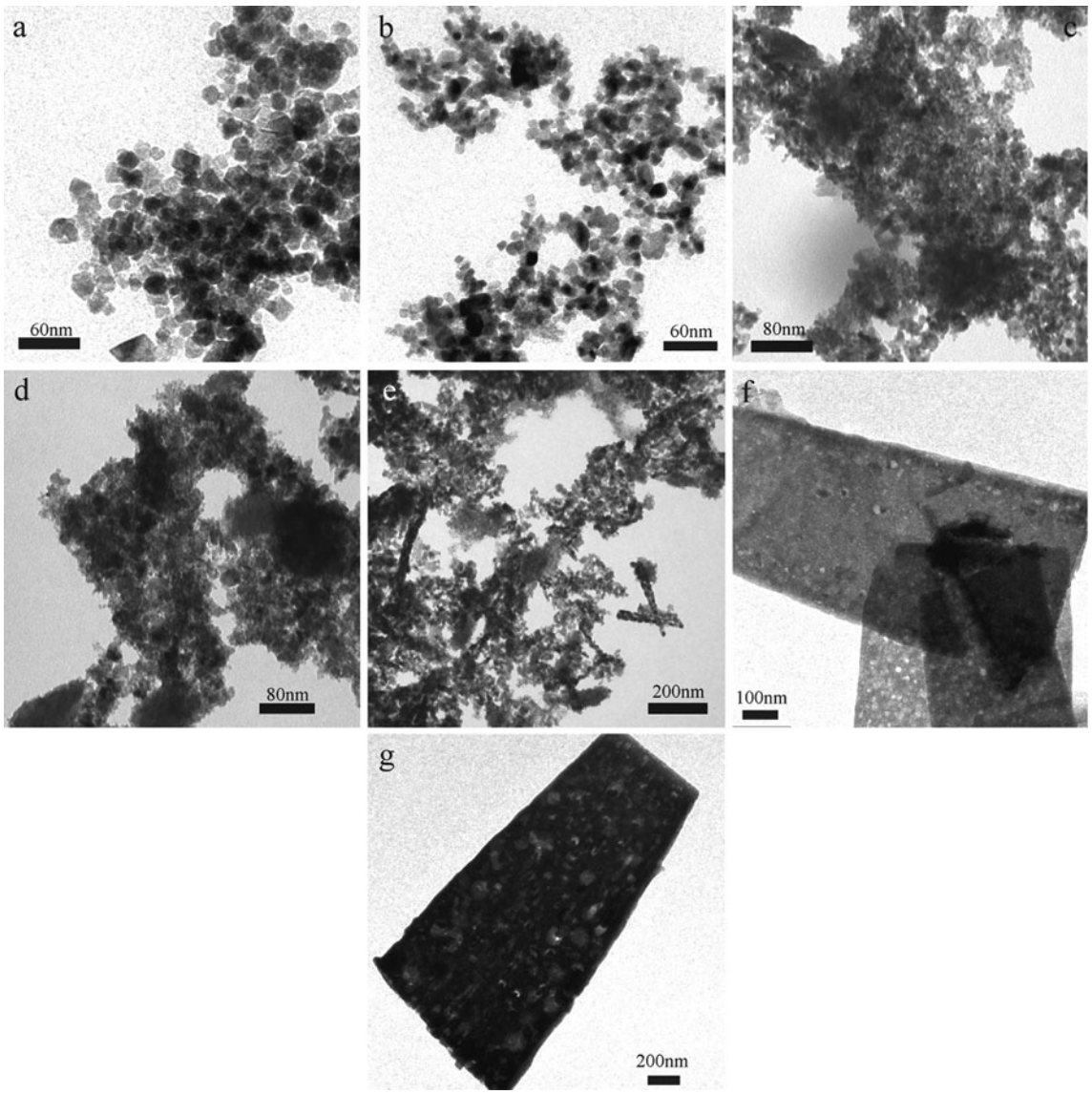

Fig. 5 TEM images of **a** Co_3O_4, **b–f** CuO/Co_3O_4 sample with Cu/Co ratio of 2:8, 5:5, 6:4, 7:3 and 9:1, respectively, **g** CuO

−1.020 V ∼ 163.48 and −1.106 V ∼ 242.29 μA, respectively in curve (3), −0.748 V ∼ 144.99, −1.029 V ∼ 314.06 and −1.108 V ∼ 435.91 μA, respectively in curve (4), as well as −0.982 V ∼ 195.06 and −1.068 V ∼ 250.55 μA in curve (5). Compared GC electrode, the electocatalytic activities for *p*-nitrophenol reduction with GC electrode modified with CuO/Co_3O_4 samples with Cu/Co ratios of 0:10, 1:9, 2:8 and 3:7, respectively were excellent. It is detected clearly that *p*-nitrophenol nearly could not been reduced at low potential (lower than −0.75 V) with GC electrode modified with CuO/Co_3O_4 samples with Cu/Co ratios of 0:10, 1:9 and 3:7, respectively, but reduction reaction could be performed on the GC electrode decorated with CuO/Co_3O_4 sample with Cu/Co ratios of 2:8 at low potentials (lower than −0.75 V), e.g. the electrocatalytic reduction for *p*-nitrophenol could be performed efficiently even at a lower potential of −0.748 V with a larger peak current of 144.99 μA using the GC electrode modified with the catalyst, and the peak current value was approximate 3.6 times bigger than that with bare GC electrode in a basic solution, and the peak potential value had decreased of 0.296 V. If electrocatalytic reduction of *p*-nitrophenol was carried out at a potential of −1.044 V, the current value with GC electrode modified with CuO/Co_3O_4 samples with Cu/Co ratios of 0:10, 1:9, 2:8 and 3:7, respectively was 2.8, 4.1, 7.9 and 5.5 times bigger than that with the bare GC electrode in basic solution. The GC electrode modified with CuO/Co_3O_4 samples with Cu/Co ratios of 5:5, 7:3, 9:1 and 10:0 were also used to investigate the electrocatalytic activities for *p*-nitrophenol reduction in a basic solution, the experiments revealed that the stability of the modified electrodes

decreased dramatically with increasing Cu/Co ratio in CuO/Co_3O_4 samples. In addition, the GC electrode decorated with CuO sample was used to investigate the electocatalytic property for *p*-nitrophenol reduction (as curve (6) in Fig. 6). Two reduction peak potentials, locating at −0.718 and −0.966 V with corresponding peak current values 87.05 and 246.53 μA, respectively, are observed. It was found in the experiments that the stability of the GC electrode modified with CuO sample was poor despite of its excellent apparent electrocatalytic activity. Thus the CuO/Co_3O_4 sample with Cu/Co ratio of 2:8 exhibits more excellent catalytic activity for *p*-nitrophenol reduction than that with the other samples.

Generally, catalyst with large specific surface area shows high electrocatalytic activity [27]. Based on Table 1, the special surface area of Co_3O_4 is 32 g/m^2, which is lower than the ones of CuO/Co_3O_4 samples with Cu/Co ratios of 1:9, 2:8, 3:7 and pure CuO (corresponding special surface area: 41, 53, 59 and 87 g/m^2, respectively), so the catalytic activity of Co_3O_4 is lowest in the five samples. Obviously, the special surface area is only the one of factors playing important roles on *p*-nitrophenol reduction. The CuO/Co_3O_4 with Cu/Co ratios of 2:8 and 3:7 almost possess the same special surface area, furthermore, CuO sample has the largest one, but the CuO/Co_3O_4 with Cu/Co ratio of 2:8 exhibits the most excellent electrocatalytic activity for *p*-nitrophenol reduction. As for the composite binary metal oxides, Cu(II) and Co(III) or Co(II) might have synergic electrocatalysis for *p*-nitrophenol reduction, which is needed to investigated in the next work.

3.6 Photocatalytic performances of samples

In this work, the resultant Co_3O_4 and CuO/Co_3O_4 samples were used as photocatalysts in the degradation for methyl orange under irradiation of incandescent lamp. The effect of irradiation time on the degradation rate of methyl orange using CuO/Co_3O_4 catalysts with different Cu/Co ratios are shown in Fig. 7. One can observe that degradation rate of methyl orange increased with increasing irradiation time with each catalyst. It is evident from Fig. 7 that the catalytic activity of composite oxides increased with increasing Cu/Co ratio in CuO/Co_3O_4 samples. As the irradiation time lasted for 60 min, the degradation rate of methyl orange was 16.8, 35.4, 40.9, 54.1, 80.5, 91.3 and 87.9% when Co_3O_4, CuO/Co_3O_4 samples with Cu/Co ratios of 5:5, 6:4, 7:3, 8:2, 9:1 and pure CuO product were used, respectively. It also can be seen from Fig. 7 that if the methyl orange solution was irradiated for a long enough time, e.g. for 120 min, the degradation rate of methyl orange all exceeded 93% using the samples except for Co_3O_4 as catalysts. Of the samples, the composite oxides with Cu/Co ratio of 9:1 and pure CuO showed more excellent catalytic activity for the degradation of methyl orange, 97.6 and 96.4% methyl orange respectively could be degraded when the degradation reaction was lasted only for 80 min. According to the TEM images shown in Fig. 4f and g, the two samples were composed of nanosheets with numerous micropores and possessed larger specific surface areas (82 and 87 g/m^2, respectively, from Table 1), which indicated the samples had higher catalytic activity.

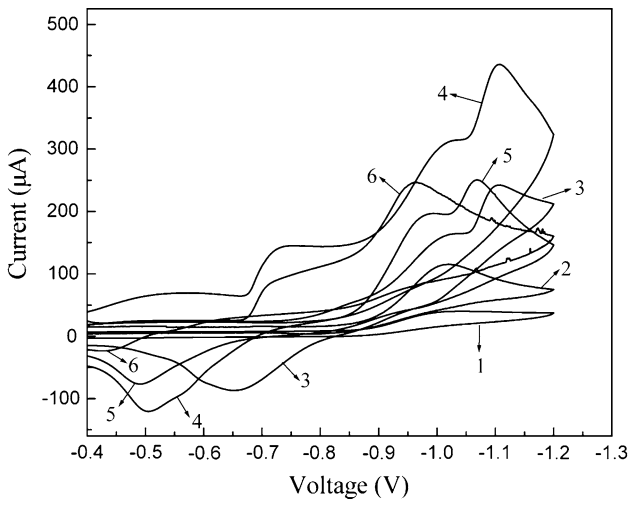

Fig. 6 Cyclic voltammorgrams of bare GC electrode (1), GC electrode modified with Co_3O_4 (2), GC electrode modified with CuO/Co_3O_4 samples with Cu/Co ratios of 1:9 (3), 2:8 (4), 3:7 (5) and CuO (6) respectively, in 1.0 mol L^{-1} sodium hydroxide +1.0 mol L^{-1} *p*-nitrophenol (scan velocity 0.02 $V.s^{-1}$)

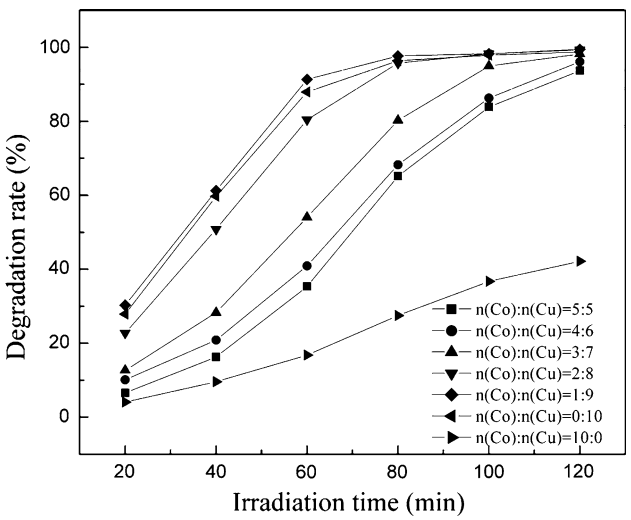

Fig. 7 Effect of irradiation on the degradation of methyl orange using CuO/Co_3O_4 catalysts with different Cu/Co ratios

The CuO/Co_3O_4 samples with Cu/Co ratios of 0:10, 1:9, 2:8, 3:7 and 4:6 as catalyst were used in the degradation of methyl orange. The experiments revealed that the degradation rate of methyl orange was low even the irradiation time lasted for 120 min, indicating the samples could not utilized visible light efficiently and showed poorer catalytic activity for the degradation of methyl orange. Thus, we speculated that it was favorable to degrade methyl orange with the CuO/Co_3O_4 sample with a higher Cu/Co ratio. As *p*-type semiconductors, CuO and Co_3O_4 have different band gaps, CuO with 1.21 eV but Co_3O_4 with 2.19 eV, which indicates that CuO utilizes visible light more efficiently than Co_3O_4 which leads to different photocatalytic activity under irradiation of visible light.

The above experiments suggested that the CuO/Co_3O_4 product with Cu/Co ratio of 9:1 exhibited most excellent photocatalytic activity than the other as-obtained samples for methyl orange degradation. Table 2 displays the effect of catalyst concentration on the degradation of methyl orange using the catalyst with Cu/Co ratio of 9:1 when the irradiation time was controlled for 80 min. With decrease of the catalyst concentration from 0.5 to 0.1 g L^{-1}, the degradation rate of methyl orange almost kept constant, and it only decreased 0.9% (from 98.7 to 97.8%). Further decreasing the catalyst concentration to 0.05 g L^{-1}, the degradation rate of methyl orange only decreased a little (from 97.8 to 92.8%), indicating that a lower concentration of the catalyst with Cu/Co ratio of 9:1 still showed higher catalytic activity.

To investigate the mechanism of photocatalytic degradation of methyl orange, no H_2O_2 was added to the reaction system in the controlled experiments. The results are shown in Table 3. As can be seen from Table 3, when methyl orange solution was irradiated for 20 min, the degradation rate of methyl orange was only 9.1%, further prolonging the irradiation time to 120 min, the degradation rate of methyl orange almost kept constant (varying from 9.1 to 10.1%). As the comparison experiments, the methyl orange solution was irradiated by an incandescent lamp with addition of H_2O_2 but without addition of any catalyst. The results are shown in Table 4. Without addition of the catalyst, the degradation rate of methyl orange was very low, and it was only 6.3% even the irradiation time was 120 min. Based on the Tables 2, 3, and 4, we could speculated that the important degradation processes for methyl orange were involved in the following:

Table 2 Effect of catalyst concentration on the degradation rate of methyl orange

Catalyst concentration (g L^{-1})	0.05	0.1	0.2	0.3	0.4	0.5
Degradation rate (%)	92.8	97.8	98.2	98.4	98.5	98.7

The catalyst with Cu/Co ratio of 9:1 was used, and irradiation time was 80 min

Table 3 Effect of irradiation time on the degradation rate of methyl orange without addition of H_2O_2

Irradiation time (min)	20	40	60	80	100	120
Degradation rate (%)	9.1	9.9	10.1	10.1	10.1	10.2

Table 4 Effect of irradiation time on the degradation rate of methyl orange without addition of catalyst

Irradiation time (min)	20	40	60	80	100	120
Degradation rate (%)	3.8	5.9	6.0	6.2	6.3	6.3

$$\mathrm{SC(semiconductor\,catalyst)} + h\nu \rightarrow \mathrm{SC}(h^+_{vb}, e^-_{cb}) \rightarrow \text{recombination} \quad (1)$$

$$2H_2O_2 + h^+_{vb} \rightarrow HO + H_2O + H^+ \quad (2)$$

$$HO + HO \rightarrow H_2O + 1/2\,O_2$$

$$HO + H \rightarrow H_2O(\text{recombination}) \quad (3)$$

$$H^+ + e^-_{cb} \rightarrow H$$

$$H + H \rightarrow H_2.$$

Degradation of methyl orange by $HO^{\bullet}$ radical

$$HO + \text{methyl orange} \rightarrow CO_2 + H_2O. \quad (4)$$

Under irradiation of visible light, water is difficult to split by the visible light with lower energy and almost no HO• radical can be obtained even at the catalysis of semiconductor. So the degradation rate of methyl orange is very low (less than 11%) under the irradiation of visible light for 120 min. With addition of the catalyst, a great deal of HO•radicals can be produced by the decomposition of H_2O_2 under irradiation of visible light, leading to significant degradation of methyl orange.

Although the above experiments indicated that the CuO/Co_3O_4 sample with Cu/Co ratio of 9:1 had shown higher photocatalytic activity in the degradation for methyl orange, it was not confirmed if it could be reused for many times. The Table 5 shows the repeatability of CuO/Co_3O_4 catalyst with Cu/Co ratio of 9:1. Each degradation reaction was carried out for 80 min. After being used for eight times, the catalyst still exhibited high catalytic activity, furthermore the degradation rate of methyl orange almost kept unchangeable in each experiment.

Table 5 Repeat ability of the catalyst with Cu/Co ratio of 9:1

Recycle times	1	2	3	4	5	6	7	8
Degradation rate (%)	98.6	98.4	98.5	98.6	98.3	98.3	98.2	97.4

4 Conclusions

In the work, the as prepared Cu-Co composite oxides with Cu/Co ratios ranging from 0:10 to 3:7 decorated on GC electrode showed excellent electrocatalytic activity for the *p*-nitrophenol reduction in the basic solution. Of the samples, the one with Cu/Co ratio of 2:8 exhibited the highest catalytic activity, for the *p*-nitrophenol could be reduced efficiently at a lower potential (decrease of 0.296 V) but with a 3.6 times bigger current compared with the bare GC electrode. The samples with Cu/Co ratios from 5:5 to 10:0 demonstrated high photocatalytic activities for methyl orange degradation under the irradiation of visible light. When the samples whose concentration was 0.5 g L^{-1} was used, the degradation rate of methyl orange all exceeded 93% under the irradiation for 120 min. In comparison, the sample with Cu/Co ratio of 9:1 exhibited the highest catalytic activity for the degradation of methyl orange, and the degradation rate could reach 97.6% even by the irradiation for 80 min, furthermore, when its concentration decreased from 0.5 to 0.1 g L^{-1}, the degradation rate of methyl orange almost kept unchanged under the same time of irradiation. The sample with Cu/Co ratio of 9:1 showed high repeatability and the degradation rate of methyl orange was almost invariable after it had been used for 8 times under the other conditions were fixed. The samples with different Cu/Co ratios have potential applications in electrocatalysis and photocatalysis.

References

1. M.K. Wu, J.R. Ashburn, C.J. Torng, P.H. Hor, R.L. Meng, L. Gao, Z.L. Huang, Y.Q. Wang, C.W. Chu, Phys. Rev. Lett. **58**, 908 (1987)
2. K.L. Hardee, A.J. Bard, J.Electochem. Soc. **124**, 215 (1977)
3. S. Nakayama, A. Kimura, M. Shibata, S. Kuwabata, T. Osakai, J. Electochem. Soc. **148**, 467 (2001)
4. K. Nagase, Y. Zhang, Y. Kodama, J. Kakuta, J. Catal. **187**, 123 (1999)
5. J. Chen, S.Z. Deng, N.S.Xu, W.X. Zhang, X.G. Wen, S.H. Yang, Appl. Phys. Lett **83**, 746 (2003)
6. J. Tamaki, K. Shimanoc, Y. Yamada, Y. Yamamoto, N. Miura, N. Yamazoe, Sens. Actuators B. **49**, 121 (1998)
7. R. Tongpool, C. Leach, R. Freer, J. Mater. Sci. Lett. **19**, 119 (2000)
8. T. Ishihara, M. Higuchi, T. Takagi, M. Ito, H. Nishiguchi, T. Takita, J. Mater. Chem. **8**, 2037 (1998)
9. A. Gulino, G. Fiorito, I. Fragalá, J. Mater. Chem. **13**, 861 (2003)
10. S.G. Kandalkar, C.D. Lokhande, R.S. Mane, S.-H. Han, Appl. Surface Science. **253**, 3952 (2007)
11. H. Kim, D.W. Park, H.C. Woo, J.S. Chung, Appl. Catal. B. **19**, 233 (1998)
12. Y. Dong, K. He, L. Yin, A. Zhang, Nanotechnology. **18**, 435602 (2007)
13. X.W. Lou, D.D.J.Y. Lee, J. Feng, L.A. Archer, Adv. Mater. **20**, 258 (2008)
14. Y.Z. Wang, Y.X. Zhao, C.G. Gao, D.S. Liu, Catal. Lett. **116**, 3 (2007)
15. G. Federico, M.N. Marta, G. Antonella, Appl. Catalys. B. **48**, 267 (2004)
16. P. Poizot, S. Laruelle, S. Grugeon, L. Dupont, J.M. Tarascon, Nature **407**, 496 (2000)
17. B. Varghese, T.C. Hoong, Y.W. Zhu, M.V. Reddy, V.R. Chowdari, T.S. Wee, B.C. Vincent, C.T. Lim, C. Sow, Adv. Funct. Mater. **17**, 1932 (2007)
18. J. Jiang, L.C. Li, Materials Letters. **61**, 4894 (2007)
19. G. Avgouropoulos, T. Ioannides, Applied Catalysis B: Environmental. **67**, 1 (2006)
20. M.F. Luo, J.M. Ma, J.Q. Lu, Y.P. Song, Y.J. Wang, J.Catal. **246**, 52 (2007)
21. D.B. Li, X.H. Liu, Q.H. Zhang, Y. Wang, H.L. Wan, Catal. Lett. **127**, 377 (2009)
22. J. Huang, S.R. Wang, Y.Q. Zhao, X.Y. Wang, S.P. Wang, S.H. Wu, S.M. Zhang, W.P. Huang, Catal. Commun. **7**, 1029 (2006)
23. Y. Sharma, N. Sharma, G.V. Subba Rao, B.V.R. Chowdari, Journal of Power Sources. **173**, 495 (2007)
24. A.C. Tavares, M.A.M. Cartaxo, M.I.D.S. Pereira, F.M. Costa, J. Solid State Electrochem. **5**, 57 (2001)
25. Y.M. Dong, K. He, L. Yin, A.M. Zhang, Nanotechnology. **18**, 435602 (2007)
26. J. Carpentier, S. Siffert, J.F. Lamonier, H. Laversin, A. Aboukaïs, J. Porous. Mater. **14**, 103 (2007)
27. G.H. Li, C.A. Ma, J.Y. Tang, J.F. Sheng, Electrochim. Acta **52**, 2018 (2007)